

# Experimental Characterization and Theoretical Prediction of Quasi-Static Fracture Behavior of Notched ZK60-T5 Mg Samples

Jafar Albinmoussa<sup>1</sup>, Mirco Peron<sup>2</sup>, Seyed Mohamad Javad Razavi<sup>3</sup>, Mohammed Al Hussain<sup>4</sup>, Ahmed Alghanim<sup>5</sup>, and Filippo Berto<sup>6</sup>

<sup>1</sup>King Fahd University of Petroleum and Minerals

<sup>2</sup>Norges teknisk-naturvitenskapelige universitet

<sup>3</sup>NTNU

<sup>4</sup>Aalto University

<sup>5</sup>King Fahd University of Petroleum & Minerals

<sup>6</sup>Norwegian University of Science and Technology

September 16, 2020

## Abstract

Magnesium and its alloys have increasingly gained attention among practitioners and engineers due to their attractive properties, specifically their high specific strength that renders these materials suitable for several applications in different industries. However, their use is still limited, especially in load-bearing applications, due to the limited knowledge of their fracture behavior, especially in the presence of notches. The aim of this work is thus that to fill this lack, investigating the fracture behavior of notched ZK60-T5 magnesium. Eleven different notch geometries were considered, i.e. U notched specimens with notch radii of 1.5, 3, 4, 5, and 6 mm and V notched specimens with notch opening angles of 35°, 60° and 90°, and notch radii of 0.4 and 0.8 mm. The mechanical tests showed that the presence of notches reduces the ductility of the material. This was confirmed also by the fracture surface analyses carried out by means of Field Emission Scanning Electron Microscope (FE-SEM), where the size of the shear lips was shown to decrease by increasing the notch acuity. In addition, this work aims also to provide practitioners and engineers with a tool able to predict the failure loads irrespective of the notch geometry. For the first time on Mg samples, a local approach, i.e. the Strain Energy Density (SED), is used to predict the failure loads of the differently notched samples, and the results suggest high reliability of this approach, being the deviations between the experimental and the theoretical data often lower than 10%.

## Introduction

Recently, magnesium (Mg) has attracted wide interest in several applications, from biomedical to automotive sectors due to their attractive properties<sup>1-5</sup>. Particularly, the lightweight of magnesium makes this material extremely attractive for transportation industries, such as automobile and aircraft industries, due to the possibility to reduce the fuel consumption and the gas emission<sup>6</sup>. However, to fully exploit the lightweight of Mg, researchers have started focusing on the addition of alloying elements to increase the specific strength of pure Mg. In addition, if passive alloying elements are added, it is also possible to increase the poor corrosion of pure Mg<sup>7,8</sup>. Among the different Mg alloys, ZK alloys, and specifically ZK60, are particularly interesting for structural applications since the addition of Zinc and Zirconium increases the corrosion resistance of the base material and the mechanical properties (strength and ductility) due to their grain refinement effect<sup>9</sup>. However, the diffusion of these materials for structural applications is still limited due to the lack of

knowledge regarding their fracture behavior in presence of geometrical discontinuities (notches). The presence of geometrical discontinuities such as notches is in fact very common in structural components, and they are known to be detrimental for static and fatigue resistance<sup>10–13</sup>. Some preliminary works on the effect of notches on the fracture behavior of Mg alloys have been carried out. Most of the works focuses on the effect of notches on AZ alloys. Yan et al<sup>14</sup>, for example, investigating the deformation and failure behavior of AZ91 alloy found that the presence of notches decreases the ductility, similarly to what is reported in Ref. 15. Interestingly, despite decreasing the ductility, the presence of notches was found to increase the strength of AZ alloys<sup>16,17</sup>. However, these works consider only notch geometries where the notch acuity is low, while real components are weakened also by sharper notches. Additionally, to the best of the authors' knowledge, no work considers the effect of notches on ZK60 alloys. Thus, this work aims to fill this lack by investigating the fracture behavior of ZK60-T5 extruded samples weakened by eleven different notch geometries. The investigated notch geometries were such that different notch acuities and sharpness are considered, in order to cover a wider range of potential real applications. Namely, U notched specimens with notch radii of 1.5, 3, 4, 5, and 6 mm and V notched specimens with notch angles of 35, 60 and 90, and notch radii of 0.4 and 0.8 mm were considered. The mechanical properties of unnotched samples were also tested to evaluate the effects of notches on the failure behavior. In addition, the fracture surfaces were investigated by means of Field Emission Scanning Electron Microscope (FE-SEM) to understand how the different notch geometries impact on the failure mechanisms.

In addition, this work aims to overcome the other limitation hampering the widespread diffusion of Mg and its alloys in structural applications, i.e. the need for a robust design tool against failure in the presence of notches. Several criteria have been developed in the recent years to predict the fracture of different material classes (metals, ceramics, polymers), from the notch stress intensity factors (NSIFs)-based criterion<sup>18</sup> to the theory of critical distance (TCD) approach<sup>19,20</sup>. However, these criteria suffer from different drawbacks. NSIFs-based criterion, for example, is limited by its geometry dependency and by the need of evaluating accurately the stress field ahead of the geometrical discontinuities to correctly perform the fracture assessment<sup>21</sup>. The TCD approach, although overcoming the geometry limitation of the NSIFs-based criterion, is still limited by the need to evaluate accurately the stress field<sup>22</sup>. In recent years, the strain energy density (SED) approach has been reported to be a promising candidate for an easy and accurate prediction of the fracture behavior of different notched materials<sup>23–27</sup>. The SED approach, that will be described in detail in Section 3, does not suffer from the geometry dependency and from the need of evaluating accurately the stress field ahead of the geometrical discontinuities, and has therefore gained wide interest among engineers and practitioners, especially for the possibility offered to predict the failure loads of differently notched components with acceptable engineering values range between -20% and +20%. However, to the best of the authors' knowledge, the SED approach has never been applied to Mg and its alloys and we thus aim herein to fill this lack. In particular, the experimental data of the eleven differently notched ZK60-T5 specimens were compared with the predictions provided by the SED approach, showing accurate predictions, with most of the predictions characterized by a deviation of 10%.

## Material and Experiment

### Material

The material used for this investigation is extruded ZK60-T5 magnesium. The 150 mm radius cylindrical bar was acquired from SMW Engineering, Russia as 1000 mm long bar. The chemical composition of the alloy is listed in Table 1. The microstructure of the material was analyzed by preparing metallurgical samples that were polished with abrasive papers having grit sizes of 240, 320, 400 and 600. After that, the samples were etched. The etchant was prepared using 5 g picric acid, 5 ml acetic acid, 10 ml distilled water and 100 ml ethanol. Micrographic analysis of the etched samples was performed using Olympus DSX-510 digital microscope. Finally, texture analysis was carried out using Bruker D8 Discover X-ray diffractometer on the material.

## Mechanical Tests

The material was cut into rectangular blanks with their longitudinal direction parallel to the extrusion direction. Then, they were turned into cylinders with a diameter of 12 mm. Two unnotched specimens (Fig. 1a) were machined from the same blanks used for the notched specimens. These unnotched specimens are used to obtain the stress-strain curves of the material. After that, U and V notches with different sizes were introduced in the center of the specimens. The notches were machined with a depth of 3 mm. Four U-notch geometries with notch root radii of 1.5, 3, 4, 5 and 6 mm were considered. For V notch geometry, two notch root radii and three notch opening angles were considered: 0.4 and 0.8 mm, and 35, 60 and 90, respectively. Representative geometries for one U and one V notch specimens are shown in Figs. 1b and 1c. Three duplicates were tested for each distinct geometry. The unnotched and the notched specimens were tested at the same loading rate, i.e., 2 mm/min. All tests were performed using Instron 5569 frame having a loadcell capacity of 50 kN.

## Fracture Surface Analysis

Optical (OM) and scanning electron microscopes (SEM) were used to analyze the fracture surfaces of the samples. The morphology of fracture surface obtained from the tested specimens was evaluated using a Olympus DSX-CB microscope, which has a capability to perform analysis and measurement of 3D surfaces. The used field emission scanning electron microscope (FE-SEM) is FEI, Quanta FEG 250, Czech Republic.

## Theoretical background

Lazzarin and Zambardi developed the Strain Energy Density (SED) criterion, according to which, under tensile stresses, failure occurs when the average value of the strain energy density over a given control volume is equal to a critical value  $W_c$ <sup>18</sup>. According to Beltrami's hypothesis<sup>28</sup>, we have:

$$W_c = \frac{\sigma_c^2}{E} \quad (1)$$

where  $\sigma_c$  is the ultimate tensile strength and  $E$  is the Young's modulus. The critical value  $W_c$  varies from material to material but it does not depend on the notch geometry and sharpness<sup>22,29</sup>. The control volume is thought of as dependent on the ultimate tensile strength, on the Poisson's ratio  $\nu$  and on the fracture toughness  $K_{Ic}$ <sup>30</sup>. Such a method was first formalized and applied to sharp, zero radius, V-notches under mode I and mixed mode I/II loading and later extended to blunt U and V-notches and to real components<sup>21,31-36</sup>. When dealing with sharp V-notches, the critical volume is a circle of radius  $R_c$  centered at the tip (Fig. 2a).

Under plane strain conditions, the critical length  $R_c$  can be evaluated according to the following expression<sup>37-40</sup>:

$$R_c = \frac{(1+\nu)(5-8\nu)}{4\pi} \left( \frac{K_{Ic}}{\sigma_c} \right)^2 \quad (2)$$

In the case of blunt V-notches and U-notches (Figs. 2b and c, respectively), the volume assumes a crescent shape, where  $R_c$  is the depth measured along the notch bisector line. The outer radius of the crescent shape is equal to  $R_c + r_0$  where  $r_0$  depends on the notch opening angle ( $2\alpha$ ) according to the following expression:

$$r_0 = \frac{q-1}{q} \rho \quad (3)$$

with  $q$  defined as

$$q = \frac{2\pi-2\alpha}{\pi} \quad (4)$$

## Results & Discussion

### Material characterization

The microstructure of extrusion plane is shown in Fig. 3. It is seen from this figure that the microstructure is composed of grains with different sizes having an average of  $9.52 \pm 1.89 \mu\text{m}$ . This structure is commonly observed in magnesium ZK60 alloy<sup>41–43</sup>. The pole figures in Fig. 4 show that the majority of basal planes are aligned with the extrusion direction.

### Mechanical characterization

A representative monotonic tensile stress-strain curve for the material is shown in Fig. 5. According to Fig. 5, it can be seen that the material exhibits conventional power-type hardening. This is expected because it is known that the major plastic deformation mechanism is slipping when a tensile loading is applied parallel to the extrusion direction<sup>44</sup>. Magnesium exhibits distinct characteristics than conventional material such as steel and aluminum alloys due to the closed-packed hexagonal lattice structure. Because of limited slip system and depending on the loading orientation, Mg may deform plastically under slipping and/or twinning<sup>44–47</sup>. In the case of wrought Mg alloys (extruded, rolled or forged) that possess strong texture with basal planes parallel to the working direction and the c-axis normal to it<sup>48,49</sup>. Tensile loading along the working direction only activates slip mechanisms resulting in a power hardening behavior<sup>13</sup>. In particular, because basal planes (0002) can accommodate only 8% elongation, prismatic slip (1010) is also activated and becomes the dominant to accommodate additional strain reaching to 20%<sup>50</sup>. The average and the standard deviation of the mechanical properties obtained from testing two specimens are listed in Table 2.

Selected load-extension curves for the tensile tests on U and V notched specimens are shown in Figs. 6 and 7, respectively. A summary of the fracture load for these is listed in Table 3. It can be seen from Table 3 that the obtained fracture loads from the duplicates are consistent with a standard deviation between 0.02 and 1.75 kN. In addition, the effect of stress triaxiality can also be observed from the U-notch experiment that generally shows that fracture load increases as the notch root radius decreases<sup>51</sup>. In addition, notch strengthening is observed in ductile materials. Peron et al tested additively manufactured Ti-6Al-4V notched specimen using electron beam melting (EBM) process<sup>52</sup>. The authors explained that the stress triaxiality and constant effects due to elastic stress state in the bulk of the sample are contributing to the rise of the fracture load, i.e. notch strengthening, for specimens with sharper notches. However, it is noted from Figs. 6 and 7 that the relationship between notch acuity or notch sharpness and fracture load does not always hold. To illustrate, U5 specimen has less acuity than U3 or U4 but it actually has comparable fracture load them. Similarly, the fracture load for V-notch specimens with notch angle of 35 is lower than that for 60 and 90. Because the main aim of the study is to predict the fracture load of U and V notched ZK60-T5 specimens using SED method it is out of the scope to investigate the triaxiality and the notch strengthening mechanism of this material.

### SED predictions

Due to the unavailability of fracture toughness for the studied material, Eq. 2 cannot be used to evaluate the critical radius. Therefore, in these conditions, an empirical approach can be a good solution for determining the critical radius<sup>10,30</sup>.  $R_c$  can be empirically determined considering the fact that the critical strain energy density value,  $W_c$ , is independent of the acuity and shape of the notch, but it only depends on the material. Therefore, the SED of any notched geometry can be measured for different radii of the control volume, and the value of the radius at which the measured SED matches the critical one found from Eq. 1 ( $1.105 \text{ MJ/m}^3$ ) corresponds to the value of control volume measured with the critical radius,  $R_c$ .

To do so, we considered the U-notched specimen with 1.5 mm radius and we leveraged on numerical analyses by using the finite element (FE) code ANSYS to evaluate the SED. The SED values can be directly derived

from FE models, and they are mesh-independent as reported in Ref<sup>53</sup>. Axisymmetric linear elastic 2D analyses were performed (the 8-nodes axisymmetric element plane 83 was selected for these analyses). Due to the double symmetry of the geometry, only one quarter of the specimen was modeled. Symmetric boundary conditions were used for vertical and horizontal symmetry lines of the models as shown in Fig. 8. Fig. 9 plots the SED as a function of different values of the control volume and compares it with the critical SED value,  $W_c$ . It can be seen that the intersection is closed to 1.3 mm, and from a more detailed analysis where the value of the radius was varied from 1.25 mm and 1.35 mm with a step of 0.01 mm, the critical radius was found to be 1.31 mm.

Table 4 summarizes the outlines of the experimental, numerical, and theoretical findings for the tested ZK60 notched samples, except for U notched samples with 1.5 mm radius since it was used to measure the critical radius. In particular, the table summarizes the experimental stresses to failure ( $P_i$  with  $i = 1, 2, 3$ ) for every notched geometry compared with the theoretical value ( $P_{th}$ ) based on the SED evaluation. The tables also give the SED value as obtained directly from the FE models of the ZK60 samples by applying to the model the average experimental stress  $p$ . The last columns of the table report the relative deviations between experimental and theoretical stresses. As widely discussed in previous contributions<sup>31,54,55</sup>, acceptable engineering values range between -20% and +20%. As visible from the table, this range is satisfied for the great majority of the summarized test data.

The results are also given in a graphical form in Figs. 10a to 10d for the different notch geometries. The experimental values of the failure stresses (dots) have been compared with the theoretical predictions based on the constancy of the SED in the control volume (line). The plots are given for the notched ZK60 samples as a function of the notch tip radius  $\rho$ . The trend of the theoretically predicted failure stresses is in good agreement with the experimental ones.

A synthesis in terms of the square root of the local energy averaged over the control volume (or radius  $R_c$ ), normalized with respect to the critical energy of the material as a function of the notch tip radius is shown in Fig. 11. The plotted parameter is proportional to the fracture load<sup>18,30</sup>. The new data are plotted together independently of the notch geometries. The aim is to investigate the influence of the notch tip radius on the fracture assessment based on SED. From the figure, it is clear that the scatter of the data is very limited and almost independent of the notch radius, as already verified in other contributions<sup>56,57</sup>. All the values fall inside a scatter ranging from 0.8 to 1.2 with the majority of the data inside 0.9–1.1 and only one value outside the range from 0.8 to 1.2. The synthesis confirms also the choice of the control volume which seems to be suitable to characterize the material behavior under pure mode I loading. The scatter of the experimental data presented here is in good agreement with the recent database in terms of SED reported in Ref<sup>31</sup>.

## Fractography

The morphology of fracture surface obtained from the tested specimens are represented in Fig. 12. According to Fig. 12, the unnotched specimens showed a large area from the fracture surface edge toward the center of net section influenced by shear failure. These shear lips were also observable in U-notched specimens, however, their size seemed to be limited only to an area close to the specimen's surface. Finally, the presence of shear lips in V-notched specimens could not be seen in the low magnification of images obtained by the microscope. Therefore, (FE-SEM) analyses were performed on the tested specimens to study their failure mechanisms in more details. Figs. 13 to 15 show the typical fracture surfaces of the unnotched, the U-notched ( $\rho = 1.5\text{mm}$ ) and the blunted V-notched ( $2\alpha = 35$ ,  $\rho = 0.4\text{mm}$ ) specimens observed by FE-SEM. For the sake of brevity FE-SEM results from the notched specimens with highest notch acutities are presented and compared to the unnotched specimens. The fracture surfaces of the tested specimens with different geometries consist of shear lips on the area close to the edge of the fracture surface and a plateau in the center of fractured area, representing the tensile failure in this region. The shear lips follow the direction of maximum shear stress at 45, while the plateau is perpendicular to the loading direction. This morphology of the fracture surface is common among the ductile materials undergoing fibrous and shear failure mechanisms at the same time.

The observed shear lips were characterized by shear dimples. The size of these shear lips tends to decrease by increasing the notch acuity, having the largest and smallest width in the unnotched specimens and V-notched specimens of 35 opening angle and 0.4 mm tip radius (See Figs. 13a, 14a, and 15a). The smaller shear lips in the notched specimens represent the localized plastic deformation in these parts, resulting in lower ductility of the part under tensile loading and consequently reduced elongation at failure. This is in agreement with the experimental data obtained from the tensile tests. The presence of secondary cracks was detected in notched specimens. Secondary crack origins arise where the local stress concentration due to the presence of material inhomogeneities meets the intensified stress field ahead of the primary crack. The higher stress level at the vicinity of the notch together with the stress triaxiality in this region can be considered as sources for the higher appearance of these secondary cracks in the notched specimens.

The center part of the fracture surface is characterized by a mixture of both cleavage facets and dimple-like fracture features describing the mixed ductile/brittle nature of fracture in the tested specimens. Presence of secondary phase particles rich in Zn and Zr with an average size of  $5.2 \pm 2.1 \mu\text{m}$  was more evident in this region of the fracture surface (see Figs. 13f, 14f, and 15f). Due to local stress concentration around the secondary phase particles, void formation under tensile loading is more probable to occur from these sites. Similar morphology of fracture features was observed for both unnotched and notched specimens.

## Conclusions

Due to their lightweight, magnesium alloys are very attractive materials for transportation industry. Therefore, an understanding of fracture behavior of these alloys is essential. Notches are unavoidable and their presence possess a risk against structural integrity of machines. The quasi-static fracture of ZK60-T5 magnesium extrusion has been investigated for U and V notched specimens. The followings summarize the major outcomes of this research:

1. Mechanical tests show that the notch acuity is inversely related to the ductility
2. Fractographic observations indicate that the material exhibits fibrous and shear failure mechanisms that are common in ductile materials.
3. The FE-SEM fractographies confirm that increasing the notch acuity reduces the ductility as shown by the reduction of the shear lips size with the increase in the notch acuity
4. Observed secondary cracks are attributed to the presence of high stress field near the notch tip and due to stress triaxiality.
5. The strain energy density criterion was successfully used to estimate the fracture load of U and V notched specimens with different sizes and geometries.

## Acknowledgment

The authors would like to acknowledge the support of King Fahd University of Petroleum & Minerals (KFUPM) for funding this research under Internal Funded Grant, Project No. IN161044.

## References

- 1 Liu C, Ren Z, Xu Y, Pang S, Zhao X, Zhao Y. Biodegradable Magnesium Alloys Developed as Bone Repair Materials: A Review. *Scanning* . 2018;2018.
- 2 Li N, Zheng Y. Novel Magnesium Alloys Developed for Biomedical Application: A Review. *Journal of Materials Science and Technology* . 2013;29: 489–502.
- 3 Luo AA, Nyberg EA, Sadayappan K, Shi W. Magnesium Front End Research and Development: A Canada-China-USA Collaboration. In: Mathaudhu SN, Luo AA, Neelameggham NR, Nyberg EA, Sillekens WH, eds. *Essential Readings in Magnesium Technology* . Cham: Springer International Publishing; 2016:41–48.
- 4 Albinmousa J, Pascu A, Jahed H, et al. Monotonic and Fatigue Behavior of Magnesium Extrusion Alloy AM30: An International Benchmark Test in the “Magnesium Front End Research and Development Project.” In: SAE International; 2010.

- 5 Albinmousa J. Fatigue of Magnesium-Based Materials. In: *Magnesium-The Wonder Element for Engineering/Biomedical Applications* . IntechOpen; 2020.
- 6 Aghion E, Bronfin B, Eliezer D. The role of the magnesium industry in protecting the environment. *Journal of Materials Processing Technology* . 2001;117: 381–385.
- 7 Peron M, Berto F, Torgersen J. *Magnesium and Its Alloys as Implant Materials: Corrosion, Mechanical and Biological Performances* . CRC Press; 2020.
- 8 Peron M, Torgersen J, Berto F. Mg and Its Alloys for Biomedical Applications: Exploring Corrosion and Its Interplay with Mechanical Failure. *Metals* . 2017;7: 252–252.
- 9 StJohn DH, Qian M, Easton MA, Cao P, Hildebrand Z. Grain refinement of magnesium alloys. *Metall and Mat Trans A* . 2005;36: 1669–1679.
- 10 Albinmousa J, Peron M, Jose J, Abdelaal AF, Berto F. Fatigue of V-notched ZK60 magnesium samples: X-ray damage evolution characterization and failure prediction. *International Journal of Fatigue* . 2020;139: 105734.
- 11 Behravesh SB, Jahed H, Lambert S. Characterization of magnesium spot welds under tensile and cyclic loadings. *Materials and Design* . 2011;32: 4890–4900.
- 12 Xiong Y, Jiang Y. Compressive deformation of rolled AZ80 magnesium alloy along different material orientations. *J Mater Sci* . 2020;55: 4043–4053.
- 13 Albinmousa J, Jahed H, Lambert S. Cyclic axial and cyclic torsional behaviour of extruded AZ31B magnesium alloy. *International Journal of Fatigue* . 2011;33: 1403–1416.
- 14 Yan C, Ye L, Mai Y-W. Effect of constraint on tensile behavior of an AZ91 magnesium alloy. *Materials Letters* . 2004;58: 3219–3221.
- 15 Yan C, Ma W, Burg V, Chen MW. Experimental and numerical investigation on ductile-brittle fracture transition in a magnesium alloy. *J Mater Sci* . 2007;42: 7702–7707.
- 16 Pan H, Wang F, Jin L, Feng M, Dong J. Mechanical Behavior and Microstructure Evolution of a Rolled Magnesium Alloy AZ31B Under Low Stress Triaxiality. *Journal of Materials Science & Technology* . 2016;32: 1282–1288.
- 17 Kondori B, Benzerga AA. Effect of Stress Triaxiality on the Flow and Fracture of Mg Alloy AZ31. *Metall and Mat Trans A* . 2014;45: 3292–3307.
- 18 Lazzarin P, Zambardi R. A finite-volume-energy based approach to predict the static and fatigue behavior of components with sharp V-shaped notches. *International Journal of Fracture* . 2001;112: 275–298.
- 19 Louks R, Askes H, Susmel L. Static assessment of brittle/ductile notched materials: an engineering approach based on the Theory of Critical Distances. *Frattura ed Integrità Strutturale* . 2014;8: 23–30.
- 20 Ayatollahi MR, Torabi AR, Bahrami B. On the necessity of using critical distance model in mixed mode brittle fracture prediction of V-notched Brazilian disk specimens under negative mode I conditions. *Theoretical and Applied Fracture Mechanics* . 2016;84: 38–48.
- 21 Chebat F, Peron M, Viespoli L, Welo T, Berto F. Fatigue Strength Assessment of Steel Rollers: On the Reliability of the Strain Energy Density Approach on Real Components. *Applied Sciences* . 2018;8: 1015.
- 22 Peron M, Torgersen J, Berto F. Rupture Predictions of Notched Ti-6Al-4V Using Local Approaches. *Materials* . 2018;11: 663.
- 23 Ayatollahi MR, Rashidi Moghaddam M, Berto F. A generalized strain energy density criterion for mixed mode fracture analysis in brittle and quasi-brittle materials. *Theoretical and Applied Fracture Mechanics* . 2015;79: 70–76.

- 24 Salavati H, Alizadeh Y, Kazemi-Moridani A, Berto F. A new expression to evaluate the critical fracture load for bainitic functionally graded steels under mixed mode (I+II) loading. *Engineering Failure Analysis* . 2015;48: 121–136.
- 25 Lazzarin P, Berto F. Control volumes and strain energy density under small and large scale yielding due to tension and torsion loading. *Fatigue & Fracture of Engineering Materials & Structures* . 2008;31: 95–107.
- 26 Aliha MRM, Berto F, Mousavi A, Razavi SMJ. On the applicability of ASED criterion for predicting mixed mode I+II fracture toughness results of a rock material. *Theoretical and Applied Fracture Mechanics* . 2017;92: 198–204.
- 27 Gómez FJ, Elices M. Fracture loads for ceramic samples with rounded notches. *Engineering Fracture Mechanics* . 2006;73: 880–894.
- 28 Beltrami E, E. Sulle condizioni di resistenza dei corpi elastici. *Il Nuovo Cimento* . 1885;18: 145–155.
- 29 Peron M, Razavi SMJ, Berto F, Torgersen J, Marsavina L. Local strain energy density for the fracture assessment of polyurethane specimens weakened by notches of different shape. 2017;4232214223: 214–222.
- 30 Peron M, Razavi S, Torgersen J, Berto F. Fracture Assessment of PEEK under Static Loading by Means of the Local Strain Energy Density. *Materials 2017, Vol 10, Page 1423* . 2017;10: 1423.
- 31 Berto F, Lazzarin P. Recent developments in brittle and quasi-brittle failure assessment of engineering materials by means of local approaches. *Materials Science & Engineering R* . 2014;75: 1–48.
- 32 Pook LP, Berto F, Campagnolo A, Lazzarin P. Coupled fracture mode of a cracked disc under anti-plane loading. *Engineering Fracture Mechanics* . 2014;128: 22–36.
- 33 Peron M, Razavi SMJ, Berto F, Torgersen J. Notch stress intensity factor under mixed mode loadings: an overview of recent advanced methods for rapid calculation. *Frattura ed integrità strutturale* . 2017;42: 196–204.
- 34 Peron M, Torgersen J, Berto F, Peron M, Torgersen J, Berto F. A Novel Approach for Assessing the Fatigue Behavior of PEEK in a Physiologically Relevant Environment. *Materials 2018, Vol 11, Page 1923* . 2018;11: 1923.
- 35 Peron M, Katabira K, Viespoli LM, Narita F, Berto F. Mixed mode fracture behavior of notched giant magnetostrictive: Mechanical characterization and comparison among failure criteria. *Theoretical and Applied Fracture Mechanics* . 2019;99: 194–204.
- 36 Campagnolo A, Razavi SMJ, Peron M, Torgersen J, Berto F. Mode II brittle fracture: Recent developments. *Frattura ed Integrità Strutturale* . 2017;11.
- 37 Yosibash Z, Bussiba A, Gilad I. Failure criteria for brittle elastic materials. *International Journal of Fracture* . 2004;125: 307–333.
- 38 Razavi SMJ, Peron M, Torgersen J, Berto F, Welo T. 40CrMoV13.9 notched specimens under multiaxial fatigue: an overview of recent results. 2017;41322141: 440–44655.
- 39 Gallo P, Razavi SMJ, Peron M, Torgersen J, Berto F. Creep behavior of v-notched components. *Frattura ed Integrità Strutturale* . 2017;11.
- 40 Razavi SMJ, Peron M, Torgersen J, Berto F. Notched graphite under multiaxial loading. *Frattura ed Integrità Strutturale* . 2017;11.
- 41 Yu Q, Zhang J, Jiang Y, Li Q. An experimental study on cyclic deformation and fatigue of extruded ZK60 magnesium alloy. *International Journal of Fatigue* . 2012;36: 47–58.
- 42 Wang W, Zhang W, Chen W, Cui G, Wang E. Effect of initial texture on the bending behavior, microstructure and texture evolution of ZK60 magnesium alloy during the bending process. *Journal of Alloys*

*and Compounds* . 2018;737: 505–514.

43 Pahlevanpour AH, Karparvarfard SMH, Shaha SK, Behravesb SB, Adibnazari S, Jahed H. Anisotropy in the quasi-static and cyclic behavior of ZK60 extrusion: Characterization and fatigue modeling. *Materials & Design* . 2018;160: 936–948.

44 Lou XY, Li M, Boger RK, Agnew SR, Wagoner RH. Hardening evolution of AZ31B Mg sheet. *International Journal of Plasticity* . 2007;23: 44–86.

45 Barnett M. Twinning and the ductility of magnesium alloys Part I: “Tension” twins. *Materials Science and Engineering: A* . 2007;464: 1–7.

46 Staroselsky A, Anand L. A constitutive model for hcp materials deforming by slip and twinning: Application to magnesium alloy AZ31B. *International Journal of Plasticity* . 2003;19: 1843–1864.

47 Tomé CN, Kaschner GC. Modeling texture, twinning and hardening evolution during deformation of hexagonal materials. In: *Materials Science Forum* . Vol 495–497. Elsevier; 2005:1001–1006.

48 Roostaei AA, Jahed H. Role of loading direction on cyclic behaviour characteristics of AM30 extrusion and its fatigue damage modelling. *Materials Science and Engineering A* . 2016;670: 26–40.

49 Xiong Y, Yu Q, Jiang Y. An experimental study of cyclic plastic deformation of extruded ZK60 magnesium alloy under uniaxial loading at room temperature. *International Journal of Plasticity* . 2014;53: 107–124.

50 Koike J, Ohyama R. Geometrical criterion for the activation of prismatic slip in AZ61 Mg alloy sheets deformed at room temperature. *Acta Materialia* . 2005;53: 1963–1972.

51 Bridgman P. *Studies in Large Plastic Flow and Fracture: With Special Emphasis on the Effects of Hydrostatic Pressure* . Harvard University Press; 1964.

52 Peron M, Torgersen J, Ferro P, Berto F. Fracture behaviour of notched as-built EBM parts: Characterization and interplay between defects and notch strengthening behaviour. *Theoretical and Applied Fracture Mechanics* . 2018;98: 178–185.

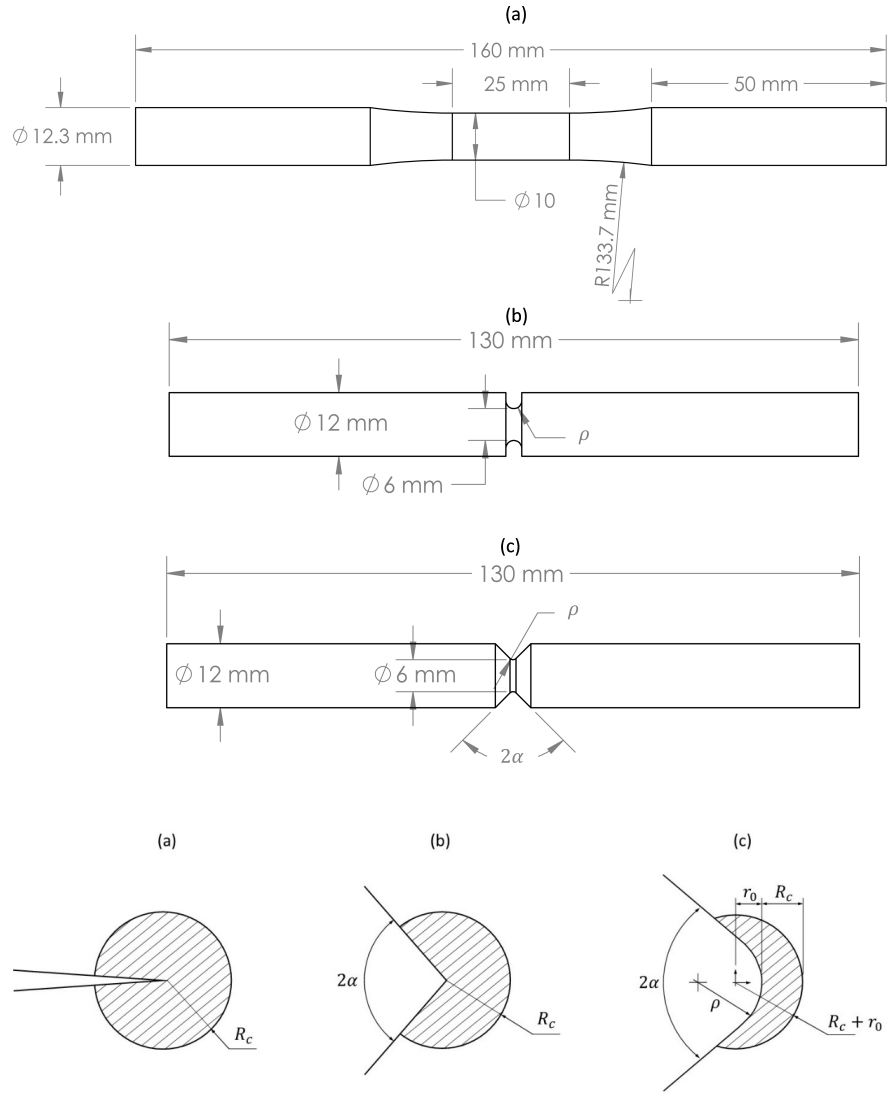
53 Lazzarin P, Berto F, Zappalorto M. Rapid calculations of notch stress intensity factors based on averaged strain energy density from coarse meshes: Theoretical bases and applications. *International Journal of Fatigue* . 2010;32: 1559–1567.

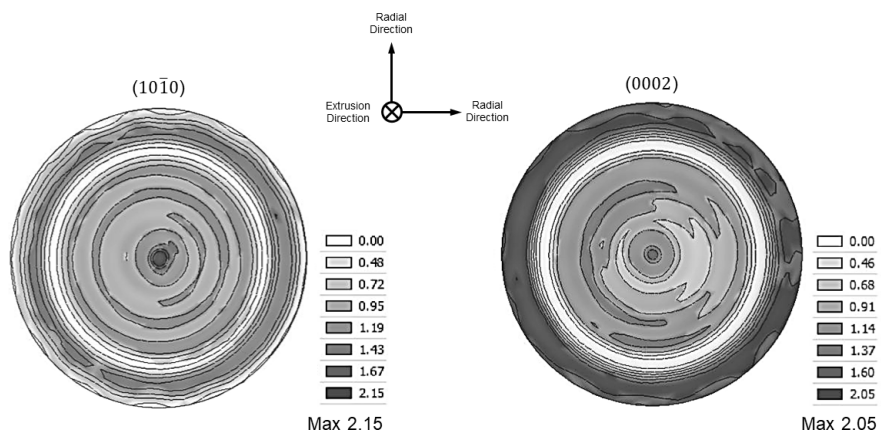
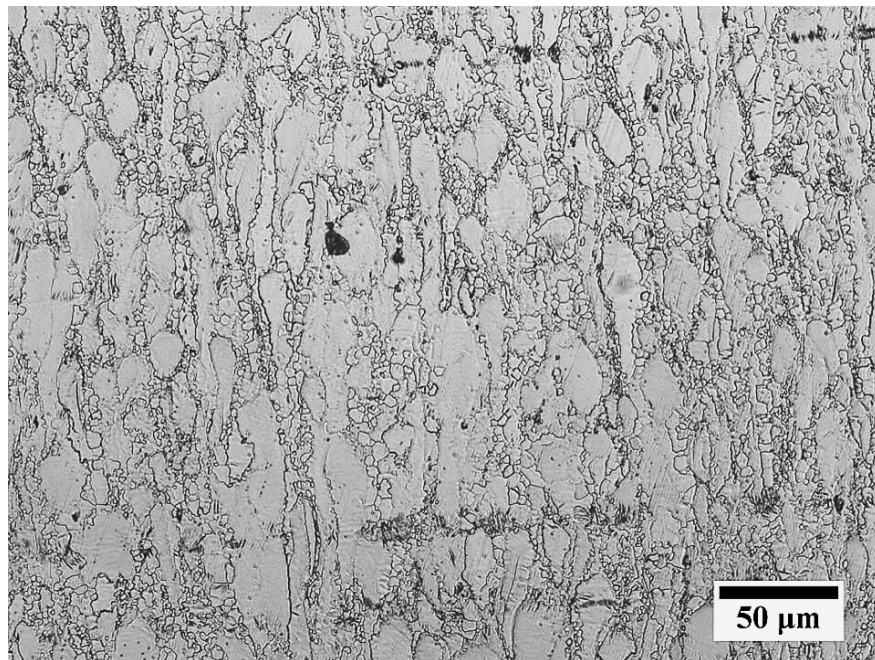
54 Torabi AR, Campagnolo A, Berto F. Mode II Brittle Fracture Assessment of Key-Hole Notches by Means of the Local Energy. *Journal of Testing and Evaluation* . 2016;44: 20140295.

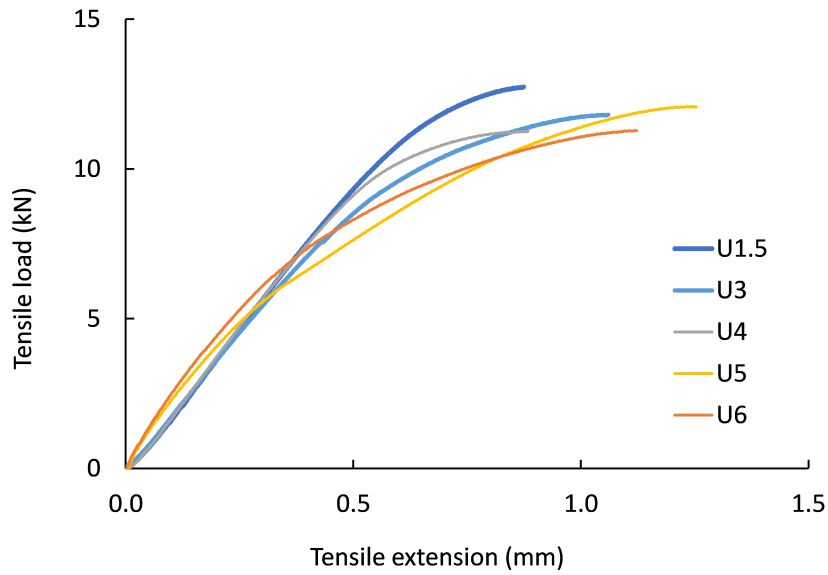
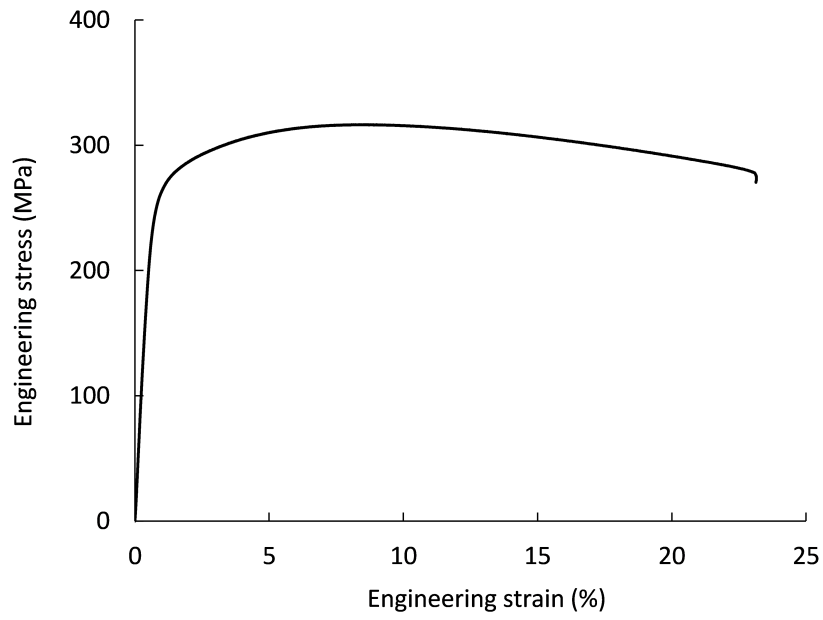
55 Berto F, Lazzarin P. A review of the volume-based strain energy density approach applied to V-notches and welded structures. *Theoretical and Applied Fracture Mechanics* . 2009;52: 183–194.

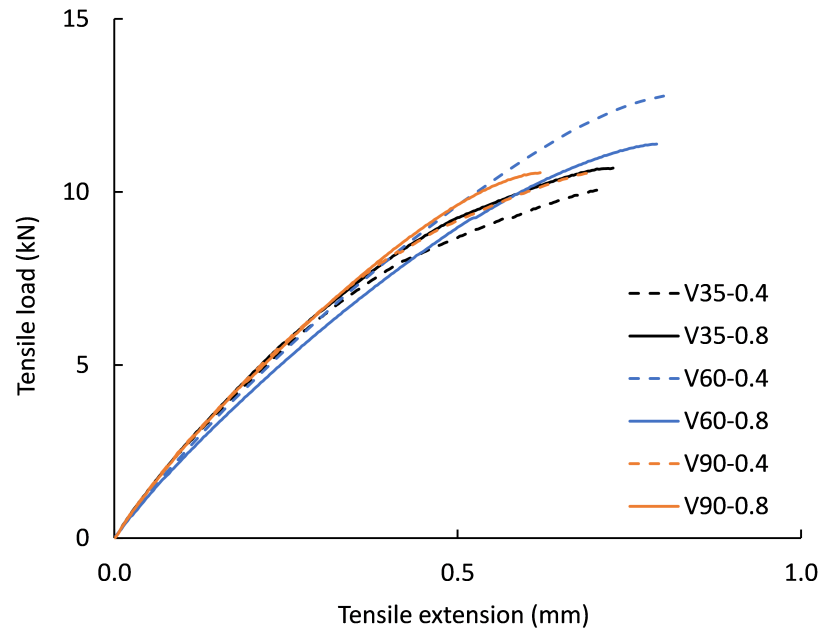
56 Gómez FJ, Elices M, Berto F, Lazzarin P. Local strain energy to assess the static failure of U-notches in plates under mixed mode loading. *International Journal of Fracture* . 2007;145: 29–45.

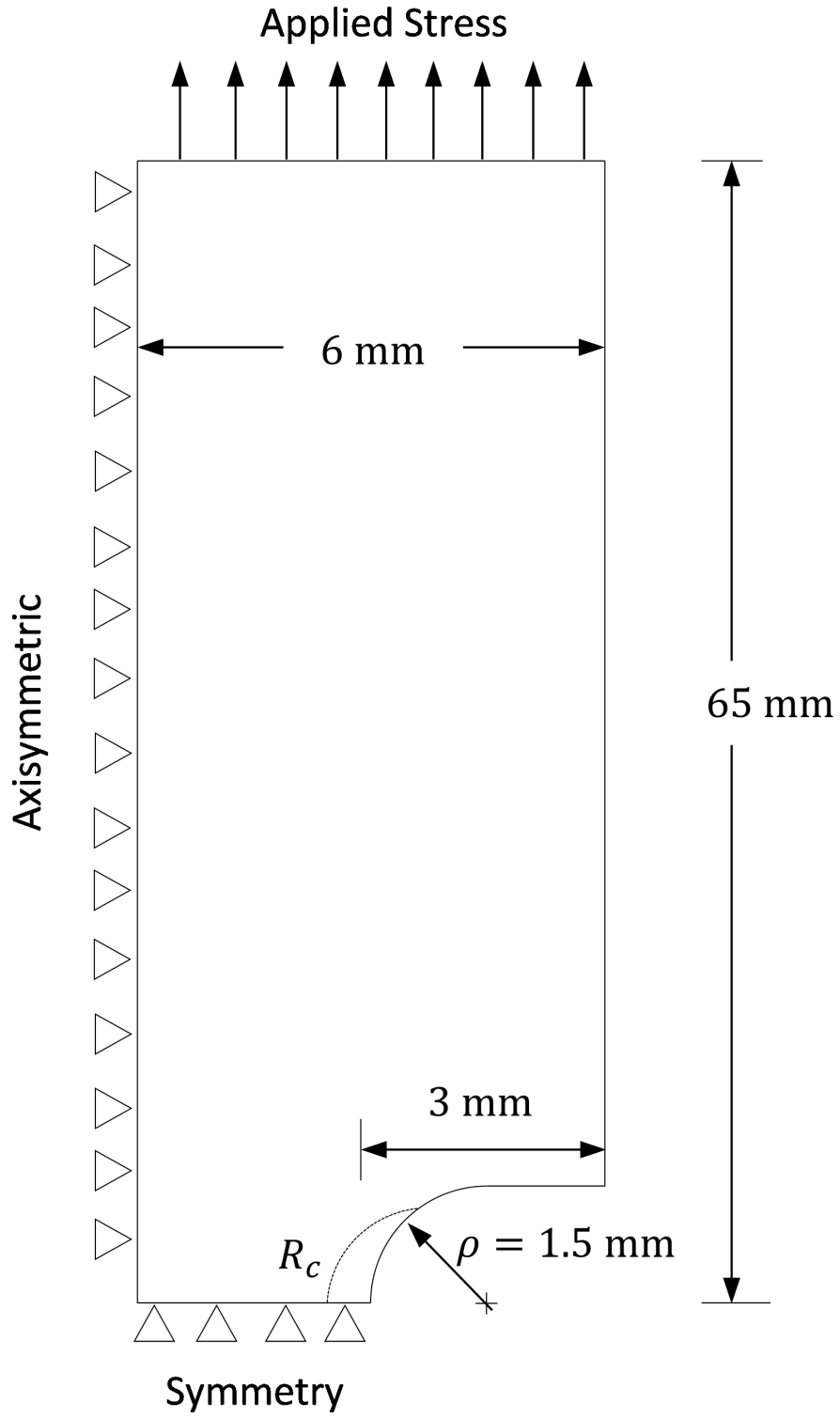
57 Lazzarin P, Berto F, Elices M, Gómez J. Brittle failures from U- and V-notches in mode I and mixed, I + II, mode: A synthesis based on the strain energy density averaged on finite-size volumes. *Fatigue & Fracture of Engineering Materials & Structures* . 2009;32: 671–684.

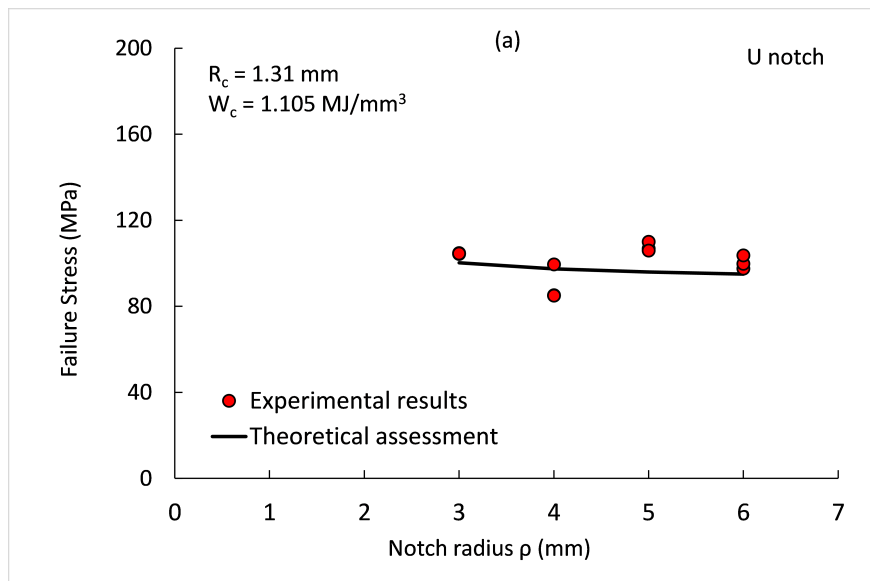
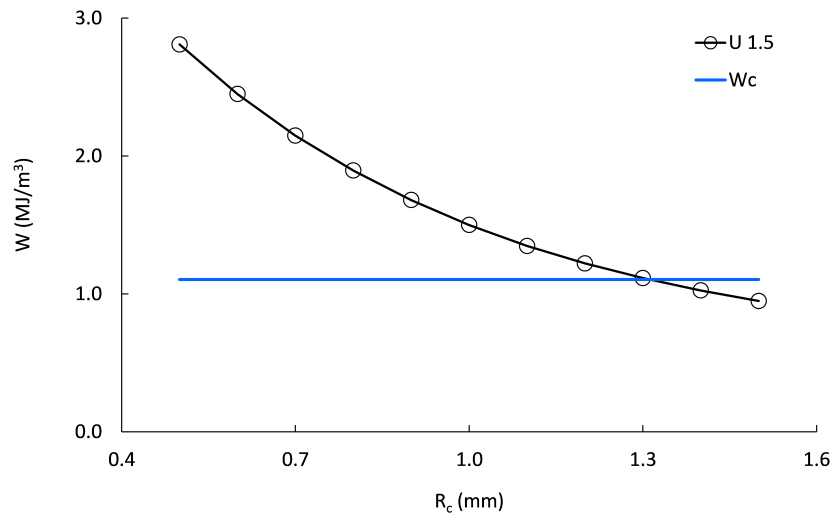


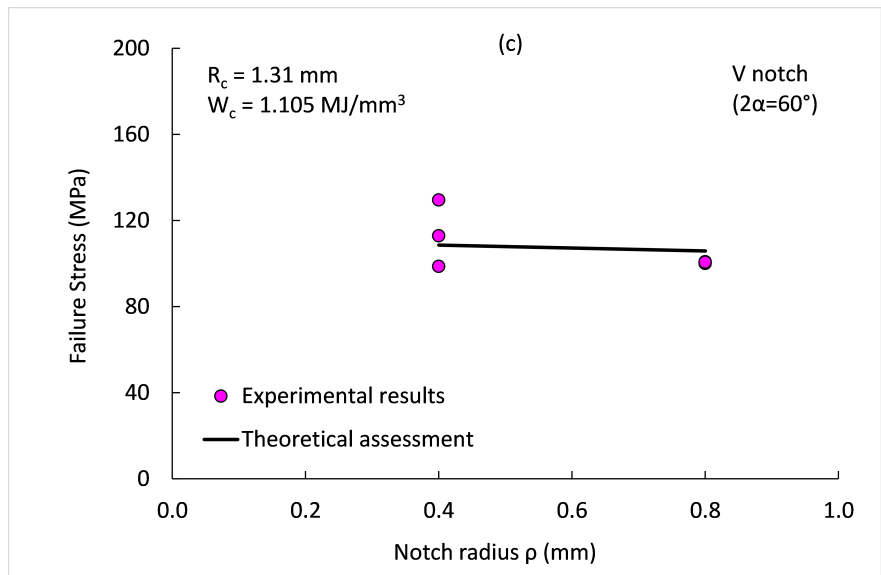
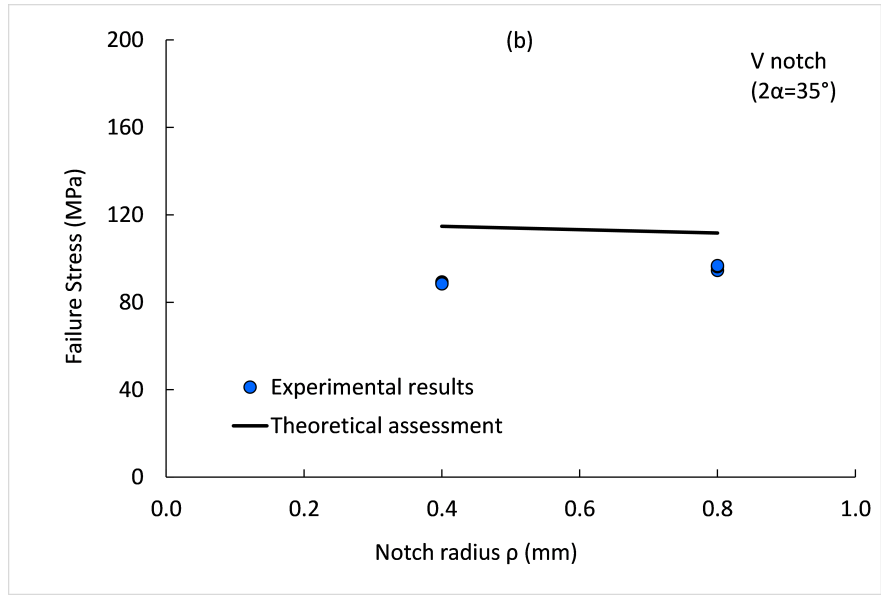


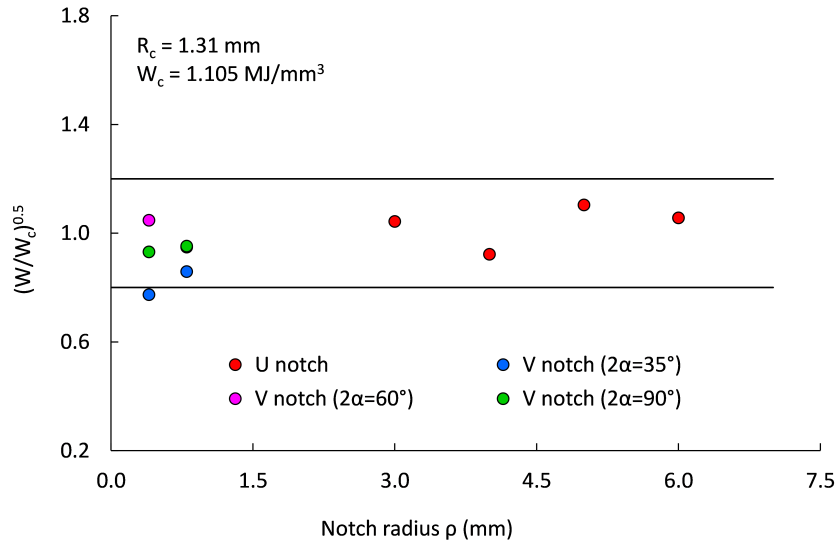
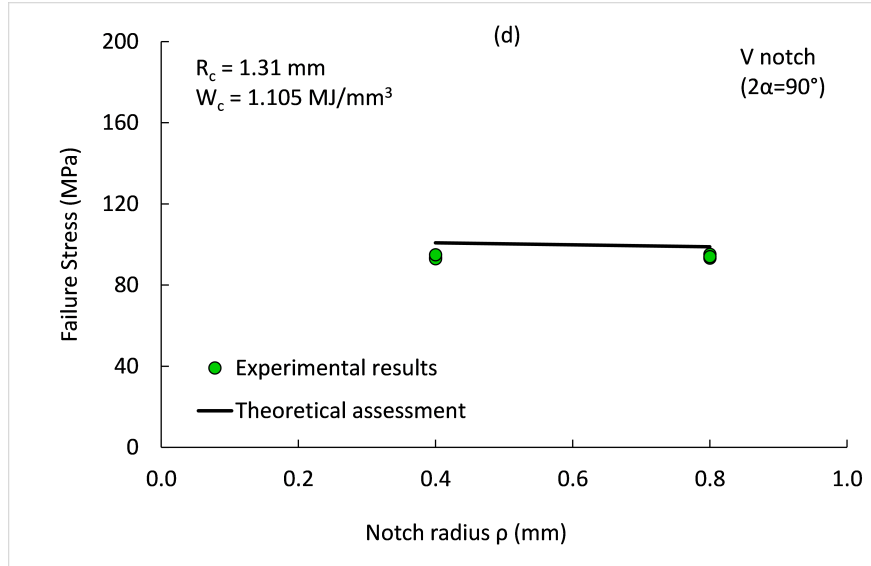


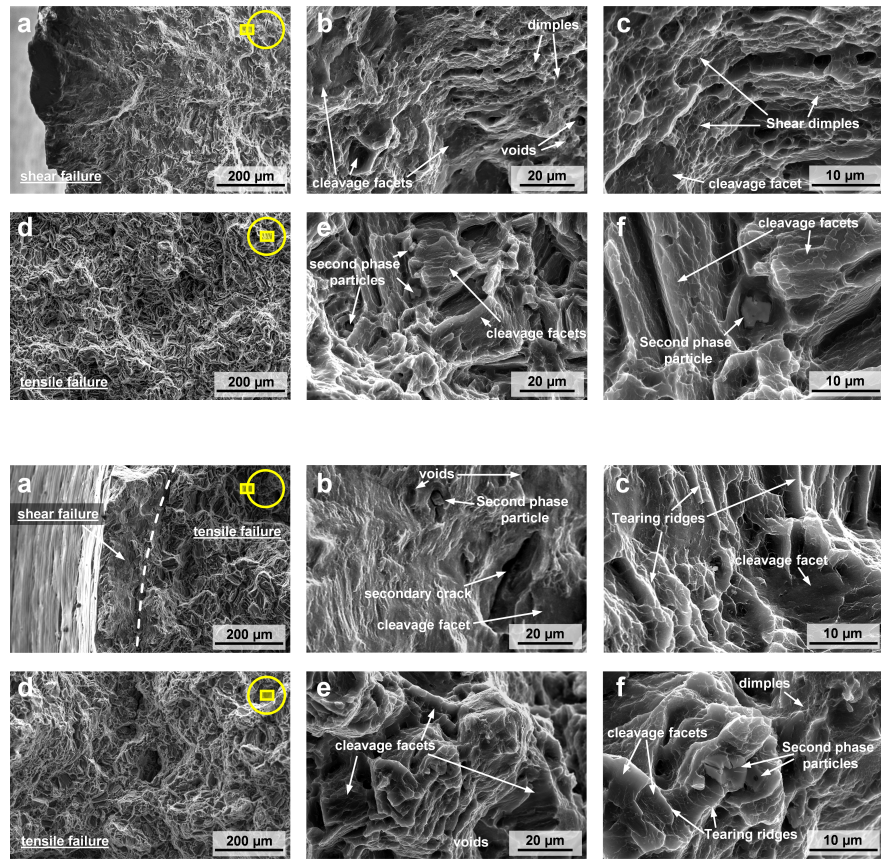
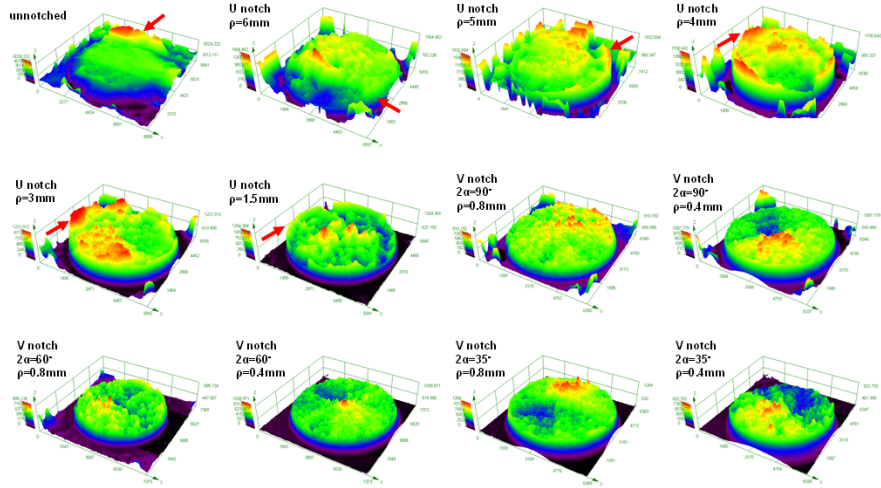


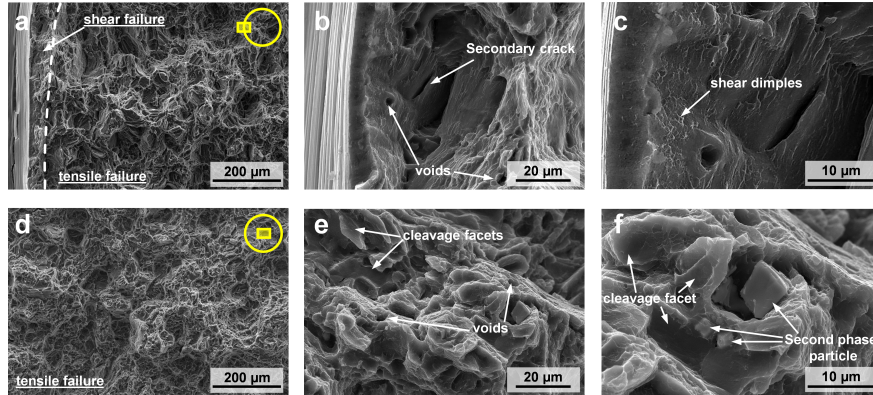












### Hosted file

Table 1.docx available at <https://authorea.com/users/359316/articles/481401-experimental-characterization-and-theoretical-prediction-of-quasi-static-fracture-behavior-of-notched-zk60-t5-mg-samples>

### Hosted file

Table 2.docx available at <https://authorea.com/users/359316/articles/481401-experimental-characterization-and-theoretical-prediction-of-quasi-static-fracture-behavior-of-notched-zk60-t5-mg-samples>

### Hosted file

Table 3.docx available at <https://authorea.com/users/359316/articles/481401-experimental-characterization-and-theoretical-prediction-of-quasi-static-fracture-behavior-of-notched-zk60-t5-mg-samples>

### Hosted file

Table 4.docx available at <https://authorea.com/users/359316/articles/481401-experimental-characterization-and-theoretical-prediction-of-quasi-static-fracture-behavior-of-notched-zk60-t5-mg-samples>